*Jurnal Teknologi*, 52 Mei 2010: 193–203


# THE ROLE OF MICROSTRUCTURES AND THE DIFFUSION OF HYDROGEN IN A PLAIN CARBON EUTECTOID STEEL FOR PRESSURE VESSELS

RONNIE HIGUCHI RUSLI[1]

**Abstract.** An electrochemical technique was used to measure the room temperature diffusivity and trapping of hydrogen in a 0.82%C steel for chemical pressure vessels in two micro structural conditions (a) the cold worked pearlitic state and (b) the hardened and tempered state. Trapping of hydrogen occurs in both structures but with more traps in the cold worked structure. Base on experimental results and observation, different hydrogen retention (trapping) behavior operates in the two structures. It was also found that patented and cold worked steels are much less susceptible to hydrogen induced embrittlement than similar steels in the hardened and tempered condition.

*Keywords:* Diffusivity of hydrogen; hydrogen embrittlement; cold-worked

## 1.0 INTRODUCTION

Most of proposed theories of hydrogen embrittlement of steels for chemical or nuclear pressure vessel (PV) assume that hydrogen segregates to regions of material where it is particularly damaging by process of fabrication procedure such as forging. Effect of irradiation strengthening and irradiation embrittlement on the transient failure of PV cladding have been observed and has been published elsewere [1–8]. In this context, it might be inferred that structure and composition of steel are more important than absolute strength [9–11]. The results of several workers support this view [12,13]. Specialty steel (patented) and cold worked steels are of special interest since there is evidence of such that for wires with this structure are less susceptible to hydrogen induced damage than are hardened and tempered materials of the same strength. This relative immunity has been recognised for some considerable time by fabricator in the past. In this investigation it was decided to examine the behaviour of a plain carbon steel in two different micro-structural conditions (i) cold worked, and (ii) hardened and tempered, both giving a nominally identical tensile strength of 1466 $MN.m^{-2}$. Delayed failure tests on notched specimens and fracture toughness tests on notched specimens confirmed the relative immunity to hydrogen embrittlement of the specialty steel and cold worked material [14,15].

[1] School of Graduate Studies, University of Indonesia Jl. Salemba 4, Jakarta 10430, Indonesia
Email: ronnie_rusli@yahoo.com

This paper deals with the results of experiment that part of the investigation concerned with the permeation of hydrogen through membranes of specialty steel sheet and cold worked 0.82%C steel and membranes of the same steel in the hardened and tempered condition. An electrochemical method of hydrogenation was used, the instrumentation and experimental procedures of which have been described elsewhere [16,17].

## 2.0 EXPERIMENTAL PROCEDURE

The base material used for this work was commercial patented and cold worked 0.82% C strip 19 mm wide × 1.0 mm thick. Chemical analysis gave its compositions as, wt. %: 0.82 C; 0.18 Si; 0.007 P; 0.55 Mn; 0.015 S; balance Fe. Specimens with a tempered martensite structure were produced from blanks of the specialty steel sheet and cold worked strip austenitised for 1.5 h at 1063° K (790°C) and quenched into whale oil at 338° K (65°C) followed by tempering for 1 h at 691° K (418°C). Mean values of the mechanical properties of 6 specimens for the two structures are shown in Table 1.

**Table 1** Mean values of the mechanical properties of the patented and cold-worked and the tempered martensite structures

| Structure | Tensile Strength ($MN.m^{-2}$) | True Fracture Stress ($MN.m^{-2}$) | Reduction in Area (%) |
|---|---|---|---|
| Patented and cold worked | 1466.1 ± 20.0 | 1943.3 ± 110.6 | 30.9 ± 3.8 |
| Tempered Martensite | 1467.9 ± 15.4 | 2075.7 ± 23.0 | 39.2 ± 1.3 |

To ensure steady state permeation rates in a reasonable time, specimens about 0.119 mm thick were used. These diaphragms were made by wet grinding blanks down to approximately 0.119 mm followed by abrading on successively finer grades of silicon carbide paper and subsequently polishing with 1 μm diamond paste. Specimens were degreased in carbon tetrachloride then washed in acetone and dried.

The permeation studies were carried out using an apparatus similar to the one described by Devanathan *et al.* [16,17]. In this method, the instantaneous rate of permeation of electrolytically charged produced hydrogen through a metal diaphragm is measured using a sensitive electrochemical technique. The apparatus consists of two cells each ending in a flanged Pyrex tube. The anodic side contains a saturated calomel

electrode terminating at diaphragm test piece. The cathodic and anodic cells on both the cathode and anode side of specimen are separated by sintered glass partitions to minimise back diffusion of oxygen from the anode since any dissolved oxygen in either solution would be reduced at the specimen surface and cause a decrease in the permeation rate.

The test specimen was placed between the two flanges and a liquid tight seal produced by using polytetrafluoroethylene washers on either side of the specimen and then clamping the flanges together. The area of the diaphragm under test was 75 $mm^2$. Oxygen-free argon gas was passed through gas lifts into the cells to achieve good circulation and also to deoxygenate both solutions. The whole apparatus was maintained at 298° K ± 0.5° K (25°C ± 0.05°C) by means of a relay and a toluene regulator in circuit with a 100 W bulb heater. An air blower was used to achieve good circulation.

Since impurities profoundly influence the uptake of hydrogen from aqueous solutions, all solutions were prepared from 'Aristar' reagents using triple distilled water. 0.05 M sulphuric acid and 0.1 M sodium hydroxide solutions were used in the cathodic and anodic compartments respectively. The solutions were initially pre-electrolysed in a divided cell for 72 hours at current density of 0.8 $mA.mm^{-2}$ and again, immediately before each determination, for a further 24 hours.

To avoid the formation of a passive film on the anodic side of the specimen surface, a thin layer of palladium was electrodeposited on the membrane surface. This was achieved by adding 10 $cm^3$ of $10^{-15}$ M palladium (as the nitride complex) to the 0.1 M sodium hydroxide in the anodic cell and electroplating the palladium from the solution at 0.025 $mA.mm^{-2}$ for 25 mins.

The specimen was maintained at a negative potential of −420 mV in opposition to a saturated calomel electrode by means of a potentiostatic circuit and was cathodically polarised using an electronically stabilised current source. The hydrogen current was monitored by measuring the IR drop across precision tin oxide resistor using a potentiometric recorder.

Each specimen was cathodically hydrogenated at a current density of 0.0165 $mA.mm^{-2}$. In order to obtain measurable permeation currents it was found necessary to add 1 $g.m^{-3}$ of arsenious trioxide to the original high purity solution.

The test procedure can be summarised as follows. The specimen diaphragm was clamped into position and the anodic cell side were filled with 0.1 M sodium hydroxide containing the palladium salt complex. Nitrogen gas was admitted to operate the gas lift to deposit palladium on the surface. A negative polarized potential of −420 mV was established and the current in the anodic circuit were recorded. When the current

had reached a steady value, the deoxygenated pre-electrolysed 0.05 M sulphuric acid were introduced into the cathodic cell. Argon gas was then admitted to the cathodic cell, while the specimen is polarised cathodically with the resulting permeation current on the anodic side monitored. When the current attained a steady value, the cathodic polarising current was switched off to allow the permeation current to decay to the background level. This procedure was repeated three times for each specimen.

The diffusion coefficients for hydrogen in the steels were determined using data from the graphical record of the rise and decay transients, as shown in Figure 1. The graphical record contains data on [17] :

(i) the break through time, $t_i$

(ii) the time lag, $t_1$. This is obtained by noting the time at which the permeation rate reached 0.63 of the steady state value, $M_\alpha$

(iii) the rise time, $t_o$

(iv) the decay time, $t_o'$

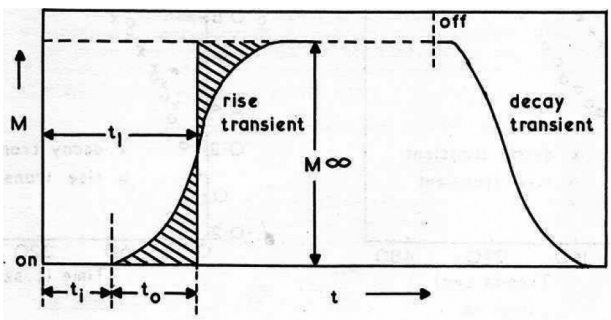


**Figure 1** Typical size and decay transients from hydrogen permeation studies

## 3.0 EXPERIMENTAL RESULTS

Figures 2 (a) and (b) and Figures 3 (a) and (b) are typical graphical records of the rise and decay transients for the first and second runs for specimens of each structure using diaphragms. The graphical record for the third run was almost invariably identical to the record of the second run. The ordinate $A$ has the value $A = M_t/M_\alpha$ for the decay transient, where $M_\alpha = DFC_o$ (where $D$ is difusivity, $F$ is the Faraday constant, $C_o$ is the concentration current at time $t$. Values of the diffusion coefficients determined are given in Table 2 (a) and (b).

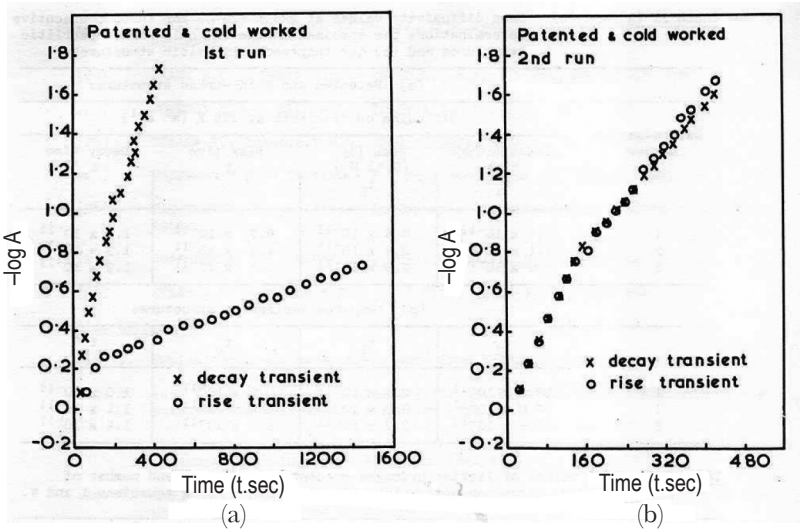


**Figure 2** (a) Graph of $\log A$ vs time ($t$) for the rise and decay transients of the patented and cold worked structure (first run) and (b) Graph of $\log A$ vs time ($t$) for the rise and decay transients of the patented and cold-worked structure (second run)

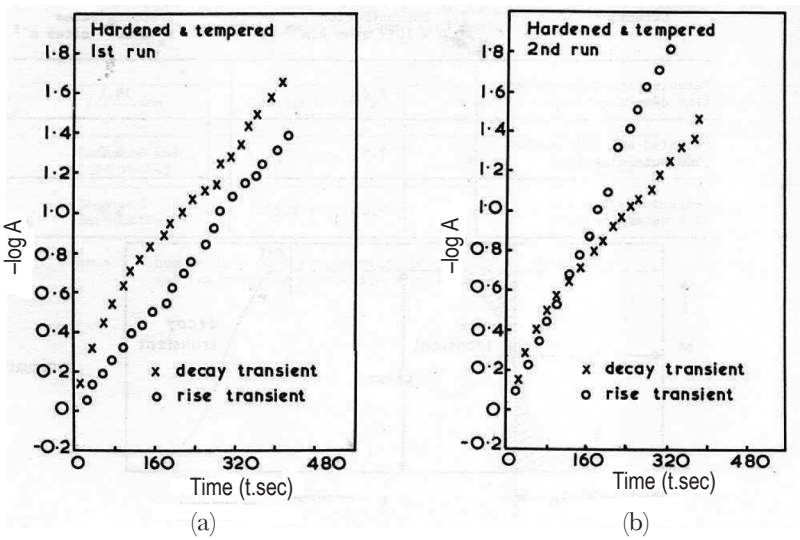


**Figure 3** (a) Graph of $\log A$ vs time ($t$) for the rise and decay transients of the hardened and tempered structure (first run) and (b) Graph of $\log A$ vs time ($t$) for the rise and decay transients of the hardened and tempered structure (second run)

The values of the diffusion coefficient obtained by the four methods of calculation show some variation although they are reasonably consistent. The mean values given in Table 2 (a) and (b) indicate a difference in diffusivity in the two structures and all the values differ by an order of magnitude from the true lattice diffusivity of hydrogen in α-iron [18,19], which at 298° K is of the order of $10^{-9}\,m^2\,s^{-1}$. It is suggested that the low diffusivity values may be attributed to trapping of hydrogen and consequently the diffusivity values are more correctly described as 'apparent' diffusivities.

Table 2 (a) and (b) shows mean diffusivity values at 298° K (25°C) for three conscutive determinations per specimen on the (a) cold worked pearlitic structures and (b) the tempered martensitic structures.

**Table 2** (a) Specialty (patented) sheet steel and cold-worked structures diffusion coefficients at 298° K ($m^2s^{-1}$)

| Determination Number | Breakthrough time, $t_i$ | Time log (0.63 $M_\alpha$) $t_1$ | Rise time $t_o$ | Rise time $t_o'$ |
|---|---|---|---|---|
| 1 | $7.4 \times 10^{-11}$ | $0.45 \times 10^{-11}$ | $0.25 \times 10^{-11}$ | $1.32 \times 10^{-11}$ |
| 2 | $7.2 \times 10^{-11}$ | $2.92 \times 10^{-11}$ | $1.40 \times 10^{-11}$ | $1.22 \times 10^{-11}$ |
| 3 | $8.2 \times 10^{-11}$ | $2.82 \times 10^{-11}$ | $1.48 \times 10^{-11}$ | $1.21 \times 10^{-11}$ |

**Table 2** (b) Specialty (patented) sheet steel and tempered martensite structures

| Determination Number | Breakthrough time, $t_i$ | Time log (0.63 $M_\alpha$) $t_1$ | Rise time $t_o$ | Rise time $t_o'$ |
|---|---|---|---|---|
| 1 | $18.71 \times 10^{-11}$ | $2.49 \times 10^{-11}$ | $0.94 \times 10^{-11}$ | $1.14 \times 10^{-11}$ |
| 2 | $17.58 \times 10^{-11}$ | $3.24 \times 10^{-11}$ | $2.26 \times 10^{-11}$ | $1.22 \times 10^{-11}$ |
| 3 | $18.17 \times 10^{-11}$ | $2.73 \times 10^{-11}$ | $1.81 \times 10^{-11}$ | $1.42 \times 10^{-11}$ |

The diffusivity data obtained from steady state permeation can be used to estimate input fugacities and lattice hydrogen concentration which may then be used to estimate the fraction of different trapping sites for hydrogen. Although many mechanisms for trapping hydrogen have been proposed, the treatment developed by Oriani [18] is consistent with the experimental results obtained in this study. According to the Oriani relationships, diffusivity is related to the time lag value ($t_1$) as:

$$t_1 = \frac{X^2}{6D_L}\left(1+\frac{3N_x}{C_{Lo}}\right) \quad (1)$$

where:

$X$ = diaphragm thickness (m).
$D_L$ = lattice diffusivity ($m^2\ s^{-1}$) = $3.3 \times 10^{-9} m^2\ s^{-1}$
$N_x$ = number of trapping sites/unit volume.
$C_{Lo}$ = lattice hydrogen concentration, atom H ($m^{-3}$).

The lattice hydrogen concentration, $C_{Lo}$, was obtained from the permeability coefficient (after Gonzales [19])

$$\varnothing = 2.92 \times 10^{-5} \exp(-8400/RT) \quad (2)$$

Which yields a value of $\varnothing = 2.02 \times 10^{-1} m^3$ (NTP.$H_2$) $m^{-1}s^{-1}bar^{-1}$at 298 K (25°C).

Fugacity was determined from the relationship,

$$j_t = \varnothing \frac{A}{X}\left(P_i^{1/2} - P_o^{1/2}\right) \quad (3)$$

Where $P_i$ and $P_o$ = the effective pressure (in bars) at the input and output sides of the diaphragm.

$A$ = area of diaphragm, ($m^2$)
$j_t$ = flow of gas normal to the surface of the diaphragm
$X$ = thickness of diaphragm, (m)

With this information the lattice hydrogen concentration may be expressed as,

$$C_{Lo} = 20.12 \times 10^{23} P_i^{1/2} \exp\left(-\frac{6500 \pm 350}{RT}\right) \quad (4)$$

The number of trapping sites/unit volume, $N_x$, can be determined using value of lattice hydrogen concentration and Equation 1. The mean values of $C_{Lo}$ and $N_x$ for three specimens of each structure are given in Table 3. A comparison of the mean values for the initial run on the two structures suggests that the cold worked pearlitic

structure has about five times more trapping sites than the tempered martensite structure.

**Table 3** Mean values of lattice hydrogen concentrations ($C_{Lo}$) and number of trapping sites per unit volume ($N_x$) determined using Equations (1) and (4)

| Structure | Mean Lattice Hydrogen Concentration $C_{Lo} \times 10^{23}$ atom H.m$^{-3}$ | Mean Number of Trapping Sites $N_x \times 10^{25}$ sites m$^{-3}$ |
|---|---|---|
| Patented and cold worked (1 st determination) | 6.78 | 19.32 |
| Patented and cold worked (2 nd determination) | 7.62 | 3.33 |
| Patented and cold worked (3 rd determination) | 7.54 | 3.82 |

## 4.0 DISCUSSION

The diffusivities shown in Tables 2 and 3 are less than the lattice diffusivity ($D_L$) of hydrogen in α-iron [18, 20] by at least an order of magnitude. Several investigators [21–23] have attributed such a decreased value of diffusivity to the impeding, or trapping of hydrogen at lattice defects such as dislocations, point defects, microvoids and various interface boundaries. On the basis of trapping phenomena, the present results indicate that trapping of hydrogen occurs, to different extents, in both the patented and cold-worked and in the tempered martensite structures. Plastic deformation, as in the case of the patented and cold worked material, introduces large numbers of defects such as dislocations [24], stacking faults [25], vacancies and interfaces [26] and microvoids [27–29].

Hydrogen permeation values obtained using breakthrough time, $t_i$, are almost independent of the permeation run number. Since the breakthrough time is obtained from the initial increase in permeation current, it will signal the arrival of the fastest diffusing species at the output side of the membrane. These diffusivity values probably reflect on the readily available lattice path for hydrogen atom diffusion between the input and output surfaces. Comparison of these diffusivities value for the two structures indicates that hydrogen diffuses more easily in the fine carbide of the tempered martensite than in the fully or partially deformed lamellar carbide of the cold worked pearlitic material. The mean values of the number of trapping sites, $N_x$, given in Table

4 corresponds to the cold worked pearlitic structure having about five times the number of sites available for trapping hydrogen than the tempered martensitic structure. For the case of the cold worked pearlitic structure, it is assumed that the second permeation run involves only the weakly trapped, then the values of $N_x$ obtained from this and subsequent permeations relates only to the number of 'weak' trapping sites. Expressed as a fraction, this means that the weak trapping sites provide only about 1/5 th of the total trap density in the cold worked pearlitic structure.

Oriani notes that consistent values of $N_x$ of the order of $10^{25}$ sites $m^{-3}$ were obtained for steels that had not been cold worked [18]. The average value of $3.72 \times 10^{25}$ and $3.24 \times 10^{25}$ sites $m^{-3}$ for the tempered martensite and cold worked pearlite (see Table 3) is in reasonably good agreement with Oriani's observation. As noted earlier, the increased in the number of structural defects due to cold-work, such as dislocations and microvoids, causes preferential retention (trapping) of hydrogen at such defects; the absence of a 'strong' trapping mode in tempered martensitic structure (typical dislocation density $10^{12}/10^{14}$ lines or $10^{-2}$ lines) suggests that a high dislocation density does not solely account for the 'strong' traps in the cold worked pearlitic structures. Although substantial metallographic effort was directed to locate and detail these 'traps', involving transmission electron microscopy of thin foils, no feature was recognized that could positively be identified as a 'strong' trap.

The dominant pattern that emerged from these permeation studies that a different hydrogen retention (trapping) behavior operates in the two structures offers a possible explanation for the established observation that patented and cold worked steels are much less susceptible to hydrogen induced embrittlement than similar steels in the hardened and tempered condition, as illustrated by delayed failure, tensile and fracture toughness tests [14,15].

## 5.0 CONCLUSIONS

(i) Trapping of hydrogen occurred in both patented and cold worked and hardened and tempered structures of the 0.8% C steel.
The cold-worked pearlitic structure had substantially more sites available for trapping of hydrogen than the tempered martensitic structure.

(ii) The cold-worked pearlitic structure contained two types of traps, one of which was a 'strong' trap than the other.

(iii) About 80% of the hydrogen traps in the cold-worked pearlitic material were 'strong or permanent' traps as a result of deformation.

## ACKNOWLEDGEMENTS

Thanks to Dr. K. Nakamura and Dr. T. Kobayashi for their support throughout the experiment, and setting up the experimentation in the laboratory during this investigation, and providing the materials for the work. This work was supported by Japan Metal and Steel Association.

## REFERENCES

[1] Basten, P. 1959. *Physical Metallurgy of Stress Corrosion Fracture.* New York: Insterscience.

[2] DiMelfi, R. J. and J. M Kramer. 1980. Irradiation Induced Strengthening and Hardening. *Journal of Nuclear Materials* 89: 338–343.

[3] Morlet, J. G., H. H. Johnson, and A. R. Troiano. 1969. Stress Induced of Hydrogen Diffusion Interstitially. *Journal Iron and Steel Institute* 189: 37–42.

[4] Zappfe, C. A. and C. E. Sims. 1941. Hydrogen Diffusion in Pearlictic Steel. *Trans. A.I.M.E* 145: 225–231.

[5] Zappfe, C. A. 1950. Hydrogen Embritlement in BCC Steel. *Materials and Methods* 32: 58–62.

[6] Petch, N. J. and P. Stables. 1952. Hydrogen Induced Hardening. *Nature*. 169(4307): 842–848.

[7] Kramer, J. M. and R. J. DiMelfi. 1981. Irradiation Hardening of Carbon Steel. *J. Nucl. Matter* 91: 321–325.

[8] Kazinczy, F. 1954. Hydrogen Induced Strees Corrosion Cracking. *Journal Iron and Steel Institute* 171: 85–91.

[9] Tetelman, A. S. 1962. Fracture of Solids. *Proceeding International Conference A.I.M.E.* 26: 671–708.

[10] Darken, L. S. and R. P. Smith. 1949. Hydrogen Permeation in BCC Steel. *Corrosion* 5: 1–9.

[11] Hill, M. L. and E. W. Johnson. 1959. Hydrogen Induced Crack Growth. *Transaction of Metallurgical Society. A.I.M.E* 215: 717–723.

[12] Frohmberg, R. P., W. J. Barnett, and A. R. Troiano. 1955. Stress Induced Difusion into Triaxial State of Stress. *Transaction of Metallurgical Society. A.I.M.E* 47: 892–902.

[13] Gray, H. R. and A. R. Troiano. 1964. Hydrogen Concentration at The Triaxial State of Stress. *Metalurgical Progress* 85: 75–84.

[14] Strecker, E. 1970. Hydrogen Gas Pressure Lowering Cohesive Strength of Interfaces. *Ph.D. Thesis*, University Manchester Institute of Science and Technology.

[15] Bartlett, R. 1973. Hydrogen Induced Crack Gowth by Stress Induced Deformation *Ph.D. Thesis*, University of Manchester.

[16] Devanathan, M. A. V. and A. Stachurski. 1962. Permeation Study in Thin Foil Steel. *Proceeding Royal Society* 270A: 90–95.

[17] Devanathan, M.A.V. 1961. Hydrogen Permeation in Stainless Steels. *Office of Naval Reseach Technical Report* 4: 71-93.

[18] Oriani, R. A. 1970. Hydrogen Diffusion in BCC Crystalline Solid. *Acta Metallurgia* 18: 147–152.

[19] Gonzales, O. D. 1969. Structural Change Induced By Hydrogen Absorption. *Transaction of Metalurgical Society, A.I.M.E* 245: 607–615.

[20] Miller, R. F., J. B. Hudson, and G. S. Ansell. 1975. Hydrogen Adsorbtion in BCC Metals. *Transaction of Metallurgical Society, A.I.M.E* 6A: 177–184.

[21] Oriani, R.A. 1967. Hydrogen in Metals, *Proceeding Symposium of Stress Corrosion*, Ohio.

[22] Frank, R. C., D. E. Swets, and D. L. Fry. 1958. The Physics Of Hydrogen Embrittlement. *Journal of Applied. Physics.* 29: 892–901.

[23] Johnson, E. W. and M. L. Hill. 1960. Hydrogen Induced stress Corrosion Cracking. *Transaction of Metalurgical Society. A.I.M.E.* 218: 1104–1112.

[24] Gibala, R. 1967. High Hydrogen Concentration in BCC Metal. *Transaction of Metalurgical Society A.I.M.E.* 239: 1574–1582.

[25] Whiteman, M. B. and A. R. Troiano. 1964. Hydrogen Induce Crack Growth in BCC Metal. *Physics of Statistical Solid.* 7: 109–114.

[26] Van Bueven. 1961. *Imperfections in Crystals*. Amsterdam: North Holland Publishing Company.

[27] Boniszewski, T. and J. Moreton. 1997. Hydrogen Induced Weld Cracking. *British Welding Journal.* 14(6): 321–329.

[28] Evans, G. M. and E. C. Rollason. 1999. Imperfection and Hydrogen Diffusion. *Journal Iron and Steel Institute*. 207: 1484–1501.

[29] Kramer, J. M. and R. J. DiMelfi. 1978. Crack Occurences In The Irradiated Steels *Journal of Nuclear Matter.* 77: 338–343.